Electronic Supplementary Material (ESI) for Journal of Materials Chemistry C.

Supporting Information

Novel Core-substituted Naphthalenediimide based Conjugated Polymer for Electrochromic Application

Kai Wang, Lin Zhu, Xuening Hu, Mingxi Han, Junyu Lin, Zhiyong Guo,* and Hongbing Zhan*

College of Materials Science and Engineering, Fuzhou University, Fuzhou 350108, Fujian, PR China.

Experimental Procedures

Materials and Instruments

All reagents and solvents were used as received from commercial suppliers without further purification. The ^{1}H and ^{13}C NMR was recorded at 298 K using Bruker Advance III 600 MHz spectrometer. Mass spectra were obtained on an Agilent 6520B spectrometer. Fourier-transform infrared spectroscopy (FTIR) was performed on a Nicolet 5700 spectrometer. X-ray photoelectron spectroscopy (XPS) was recorded directly by the coated FTO substrates using ESCALAB 250 spectrometer. All samples spectra were calibrated to sp^2 hybridized carbon at 284.6 eV in C 1s binding energy region. Scanning electron microscopy (SEM) images were obtained using a FEI Nova NanoSEM 230 at an acceleration voltage of 5 kV. Atomic force microscope (AFM) was obtained by Agilent 5500. The UV-visible (UV-vis) spectra, spectroelectrochemistry and square-wave potential step absorptiometry experiments were conducted in a quartz cuvette located in a PE Lambda 950 UV-vis spectrometer. The emission peaks and PL quantum yields were conducted on an Edinburgh FLS1000 fluorescence spectrophotometer at room temperature. Electrochemical and EIS measurements were performed with a GAMRY INTERFACE 1000 electrochemical analyser. The film thickness was measured by a Bruker Dektak XT Profilometer. DFT calculations were conducted by B3LYP/6-311G(d) basis set through Gaussian 09W program.

Cyclic voltammetry (CV) and electrochemical polymerization measurements were carried out in specifically solutions using a three-electrode electrochemical cell with an FTO-coated glass (working area about 0.8 cm × 2 cm) as the working electrode, platinum sheet as the counter electrode, and an Ag/AgCl reference electrode. The Ag/AgCl electrode was calibrated by Fc/Fc^{+} ($E_{ox,\ onset}$= 0.38 V vs Ag/AgCl). Prior to each experiment, the platinum sheets were polished carefully with abrasive paper (1500 mesh, for FTO: immersed in ethanol for 6 h and then cleaned by ultrasonic wave for 15 min), and cleaned by water and acetone successively. After the polymerization, the deposited films were washed with CH_2Cl_2 and CH_3CN for several times to remove un-reacted monomer, inorganic salts and other organic impurities for subsequent investigations. All the measurements were carried out after the solution had been purged with nitrogen for 30 minutes to avoid the effects of oxygen.

The HOMO–LUMO levels and E_g values of both three monomers are evaluated according to the empirical formulas as follows:[1]

$$\mathbf{HOMO = -(E_{ox} + 4.80)\ eV}$$

$$\mathbf{LUMO = (HOMO + E_{g,\ opt})\ eV}$$

where E_{ox} and $E_{g,\ opt}$ are the onset oxidation potential and optical bandgap, respectively.

The optical density (ΔOD) and the coloration efficiency (CE) are calculated according to the following formulas:[2]

$$\mathbf{\Delta OD = \log(T_{bleach}/T_{colored})}$$

$$\mathbf{CE = \Delta OD/Q_d}$$

where T_{bleach} and $T_{colored}$ is the maximum transmittance in the neutral and reduced states, respectively. Q_d is the ejected charge for color change.

The ionic conductivity was calculated according to the following formulas:[3]

$$\mathbf{\sigma = T/(R_{ct} \times A)}$$

where T is the thickness of the film, A is the surface area of the electrode (0.8 cm × 2 cm), and R_{ct} corresponds to the diameter of the semicircular arc.

Synthesis of DPy-NDI

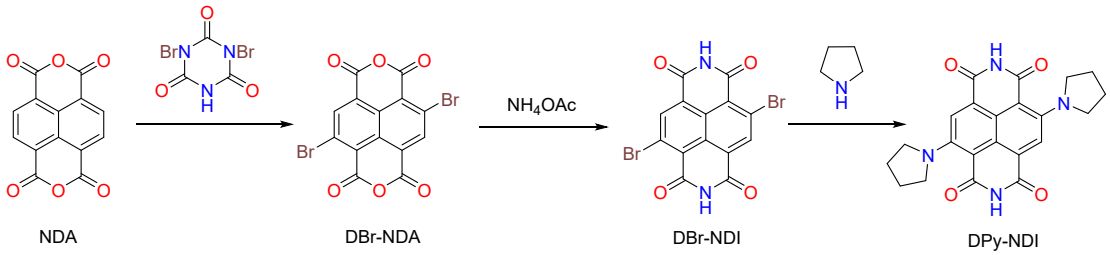

Scheme S1 General synthetic route of DPy-NDI.

DPy-NDI was synthesized from 1,4,5,8-tetracarboxylic dianhydride (NDA) in three-steps via modified literature protocols (Scheme S1)[4]. A S_NAr reaction of DBr-NDI with pyrrolidine following a literature protocol afforded DPy-NDI. Upon addition of pyrrolidine (20 mL) to yellow DBr-NDI (2.0 g, 4.7 mmol) it immediately turned dark red and then purple. The mixture was then stirred under reflux for 16 h to drive the reaction to completion. After evaporating excess pyrrolidine with a rotary evaporator, the resulting purple solid was washed successively with copious amounts of hexanes and MeOH to remove the red impurity and obtain a reasonably pure, albeit sparingly soluble DPy-NDI as a navy blue solid (1.5 g, yield ≈ 73 %).

Synthesis of DPyNDI-TPA and NDI-TPA

In order to prevent the competitive reaction, DPyNDI-TPA (Scheme S2) was synthesized by a slightly modified Cu(II)-mediated coupling reaction between 2,6-dipyrrolodinyl-NDI and corresponding arylboronic acid.

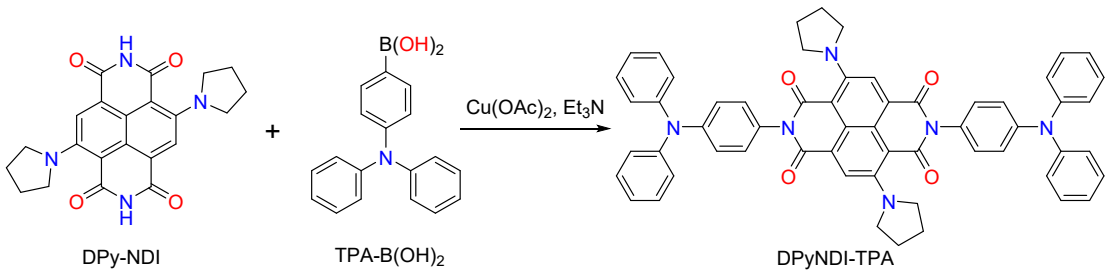

Scheme S2 Synthetic route of DPyNDI-TPA.

DPyNDI-TPA. To a suspension of DPy-NDI (0.5 g, 1.2 mmol), (4-(diphenylamino)phenyl)boronic acid (1) (3.6 g, 12.4 mmol), anhydrous $Cu(OAc)_2$ (2.2 g, 12.4 mmol), and molecular sieves (4 Å) in anhydrous DMAc (50 mL) purged with O_2 for 30 min, Et_3N (1.7 ml, 12.4 mmol) was added, and the resulting reaction mixture was stirred at 55 °C under an O_2 environment for 2 d. Additional amounts of 1 (1.8 g, 6.2 mmol), $Cu(OAc)_2$ (1.1 g, 6.2 mmol), and Et_3N (0.9 ml, 6.2 mmol) in DMAc (15 ml) were then added to the reaction mixture, which was stirred at 55 °C under O_2 environment for another 3 d. After 5 d, the reaction mixture was cooled to room temperature, and washed with CH_2Cl_2 (100 mL). After collecting the filtrate, the filtrate was extracted with water to remove residual DMAc, and the target product was dissolved in the organic phase. After concentrating the dark blue organic phase, it was purified by SiO_2 column chromatography (CH_2Cl_2/PE/EtOAc 10:10:0.7) to obtain pure DPyNDI-TPA (90 mg, yield ≈ 8.5 %) as a dark blue solid. ^{1}H NMR (600 MHz, $CDCl_3$): δ (ppm) 8.45 (s, 2H), 7.33-7.30 (t, 8H), 7.24-7.21 (m, 12H), 7.16-7.15 (d, 4H), 7.10-7.07 (t, 4H), 3.52 (t, 8H), 2.07 (t, 8H). ^{13}C NMR (151 MHz, $CDCl_3$): δ (ppm) 164.20, 161.87, 147.77, 147.55, 147.50, 129.46, 129.37, 129.32, 125.19, 125.08, 123.39, 122.96, 121.86, 105.48, 77.25, 77.04, 76.83, 52.62, 25.97. FTIR (KBr, cm^{-1}): 2967 (-CH_2-), 1654 (C=O), 1213 (C-N), 752. HPLC-Q-TOF-MS: calcd. for $C_{58}H_{46}N_6O_4$, $[M+Cl]^-$: 925.3275. Found: 925.3275.

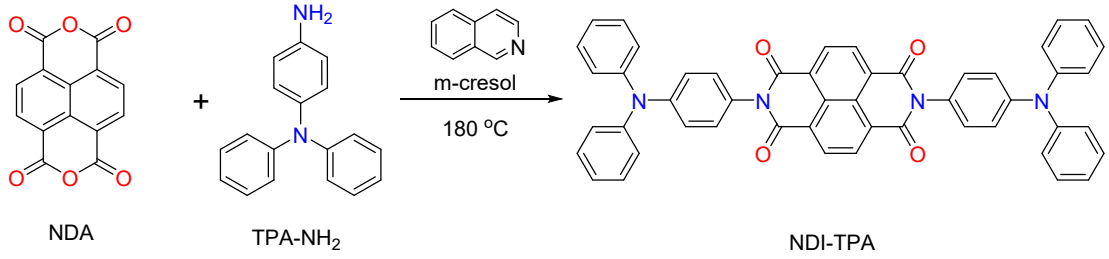

Scheme S3 Synthetic route of NDI-TPA.

NDI-TPA. NDI-TPA was synthesized according to previous literature.[5] A mixture of 520 mg (2 mmol) of TPA-NH_2 and 0.24 mg (0.9 mmol) NDA was dissolved in 10 mL of m-cresol in a 50 mL round-bottom flask. The reaction mixture was stirred at 80 °C for 2 h, and then a few drops of isoquinoline were added into the above solution. This mixture was refluxed at 180 °C under nitrogen atmosphere. After 18 h, this mixture was cooled to room temperature and poured into 150 mL of methanol. The precipitate was collected by filtration and dried to obtain pure NDI-TPA (330 mg, yield ≈ 50 %) as a purple powder. ^{1}H NMR (600 MHz, $CDCl_3$): δ (ppm) 8.87 (s, 4H), 7.34-7.32 (t, 8H), 7.25-7.22 (m, 12H), 7.19-7.17 (d, 4H), 7.12-7.10 (t, 4H).

Results and Discussion

Experimental Data

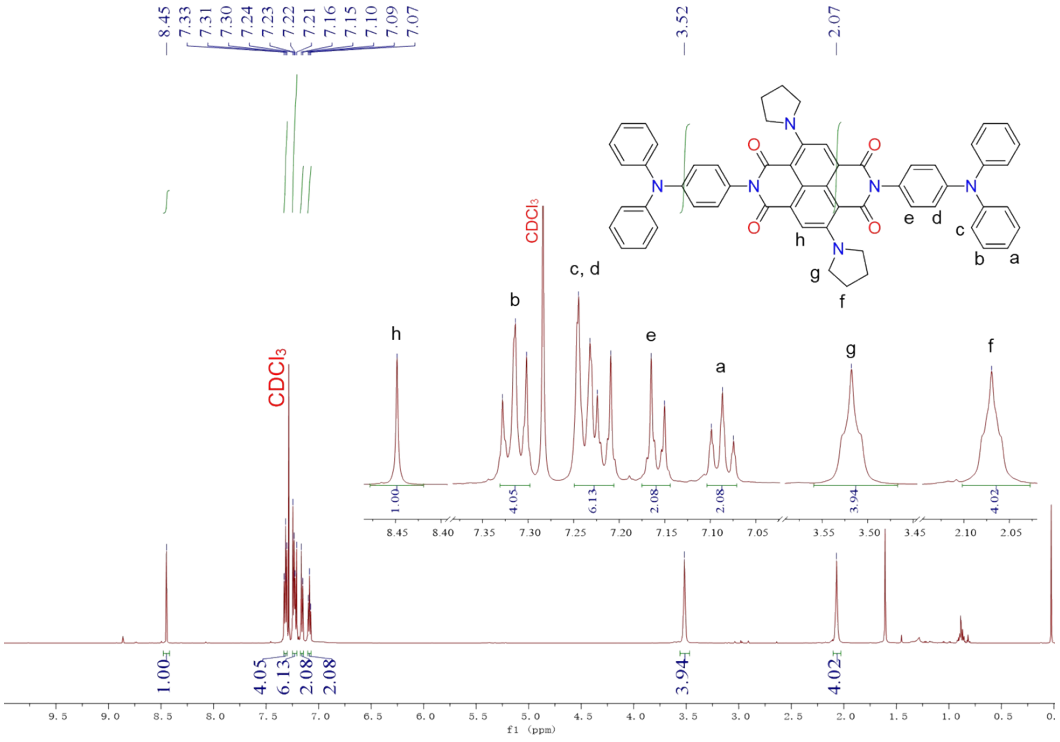

Fig. S1. ^{1}H NMR spectrum of DPyNDI-TPA in $CDCl_3$.

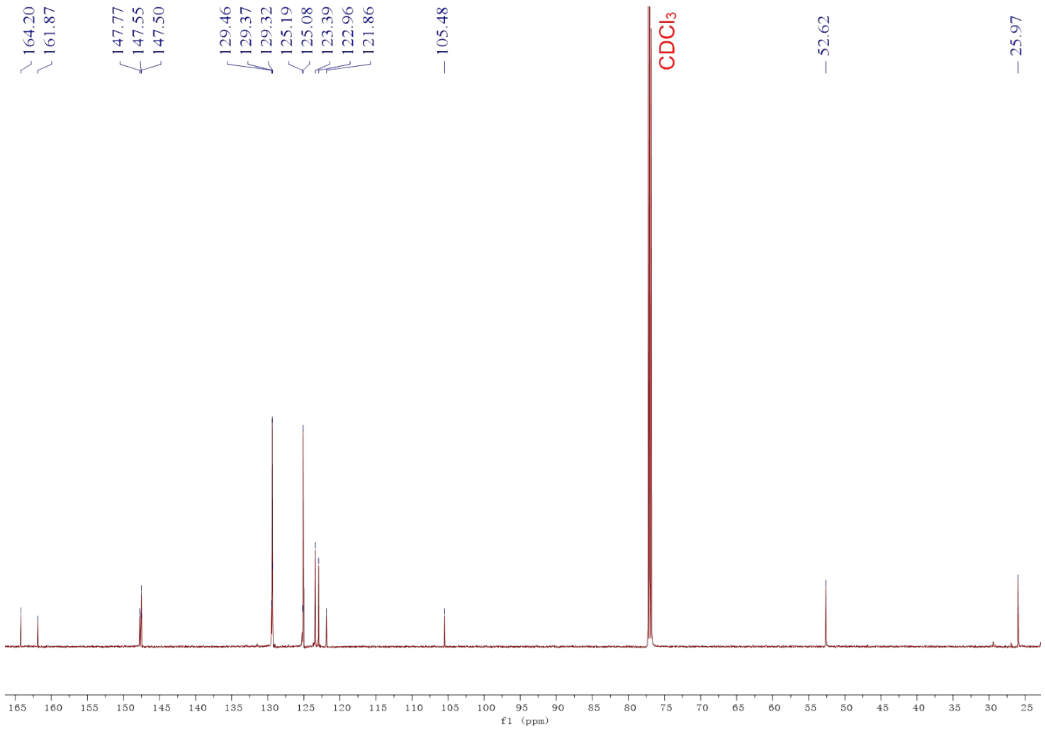

Fig. S2. ^{13}C NMR spectrum of DPyNDI-TPA in $CDCl_3$.

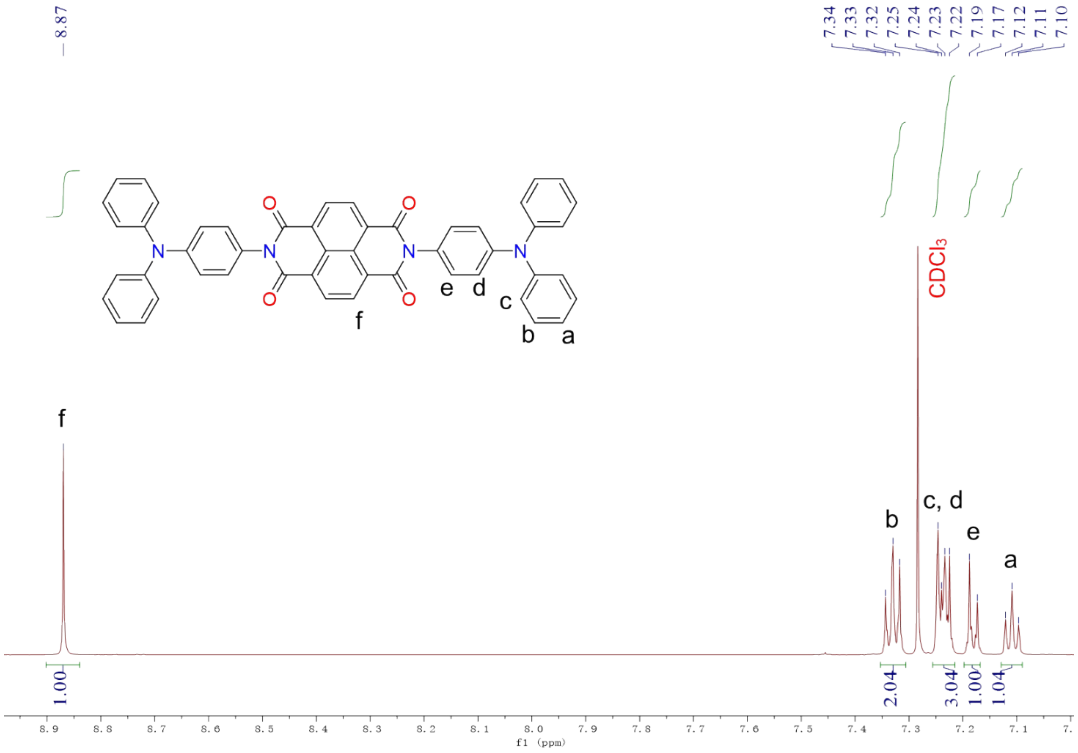

Fig. S3. ^{1}H NMR spectrum of NDI-TPA in $CDCl_3$.

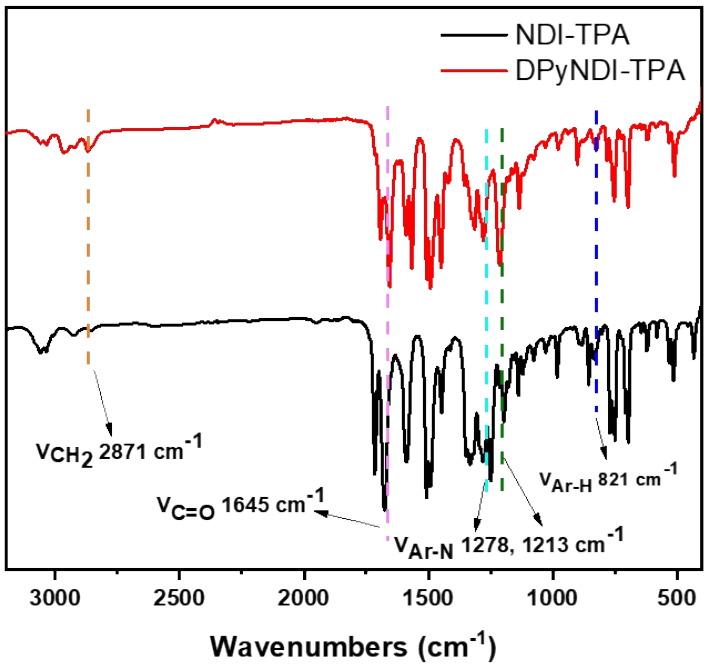

Fig. S4. FTIR spectra of NDI-TPA and DPyNDI-TPA.

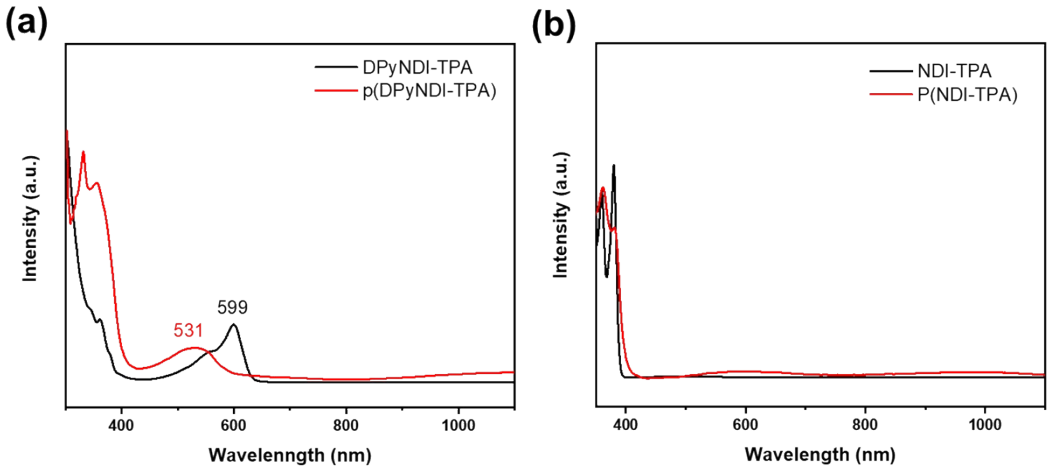

Fig. S5. (a) UV-vis-NIR spectra of DPyNDI-TPA and p(DPyNDI-TPA) film. (d) UV-vis-NIR spectra of NDI-TPA and p(NDI-TPA) film.

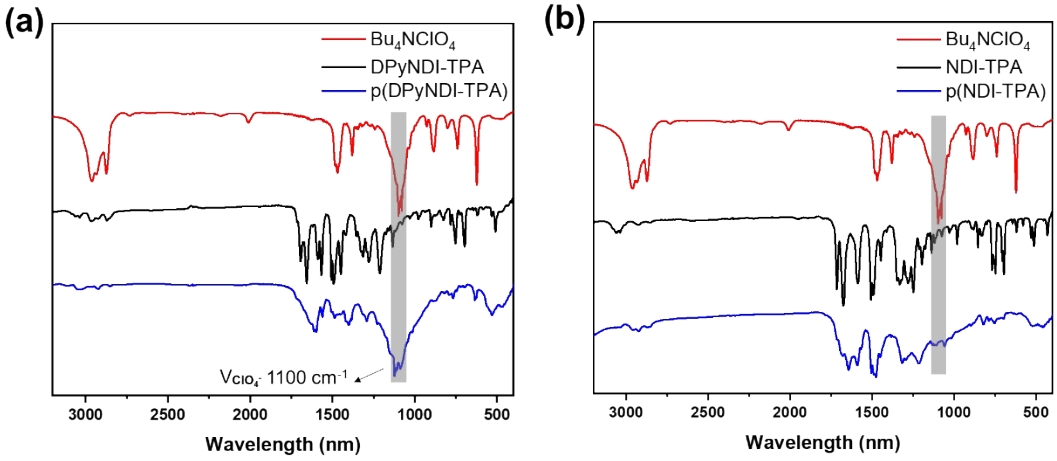

Fig. S6. (a) FTIR spectra of Bu_4NClO_4 electrolyte, DPyNDI-TPA and p(DPyNDI-TPA) film. (b) FTIR spectra of Bu_4NClO_4 electrolyte, NDI-TPA and p(NDI-TPA) film.

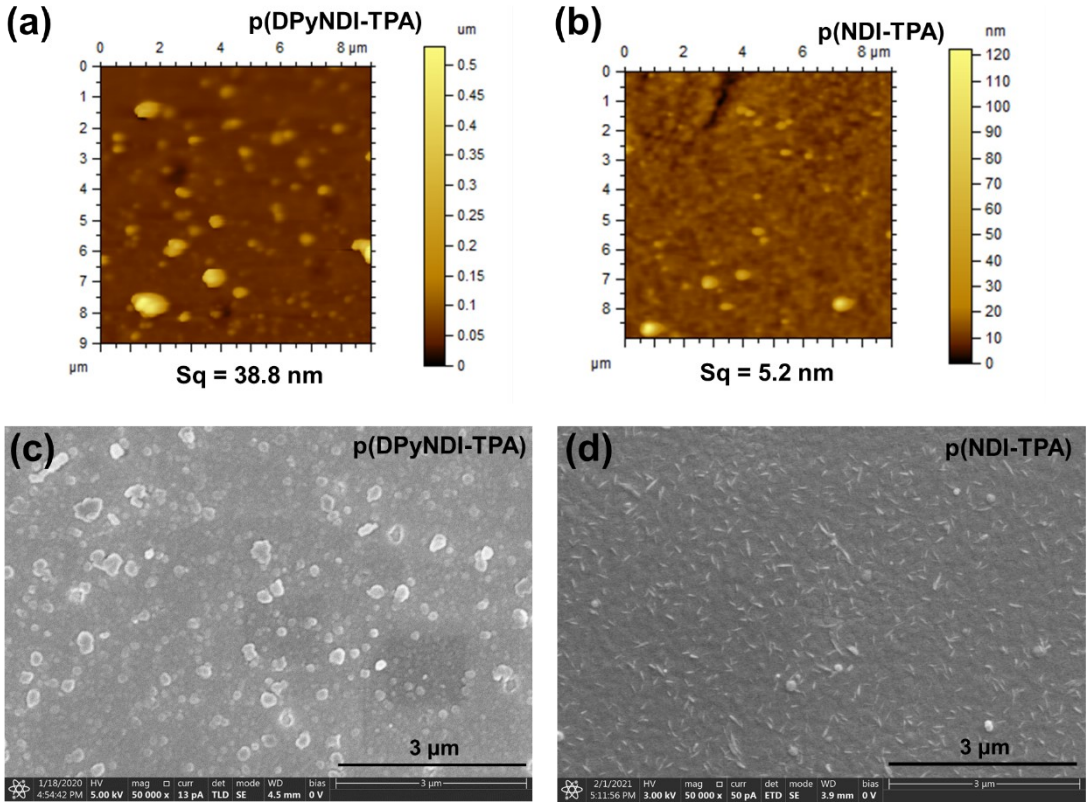

Fig. S7. (a) and (b) AFM pictures of p(DPyNDI-TPA) and p(NDI-TPA) film. (c) and (d) SEM pictures of p(DPyNDI-TPA) and p(NDI-TPA) film at different scale.

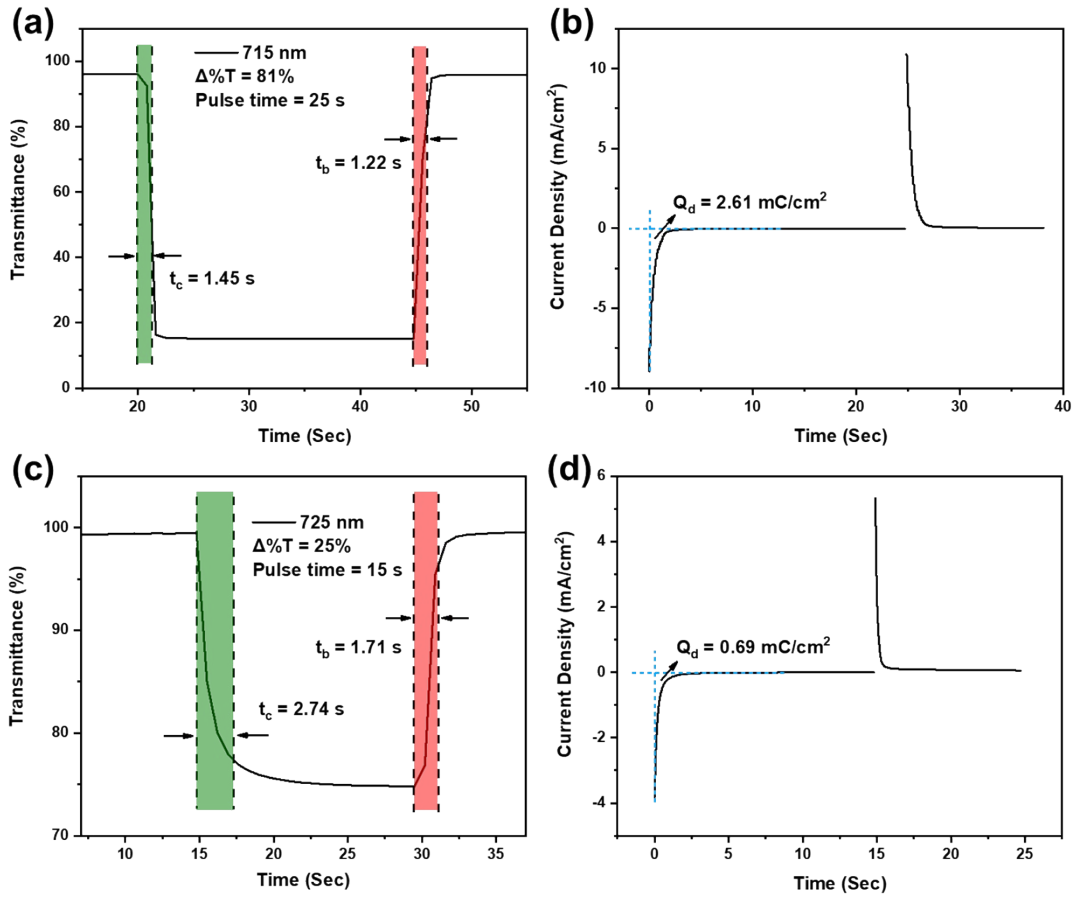

Fig. S8. (a) and (c) One cycle transmittance change of the p(DPyNDI-TPA) film at 715 nm and the p(NDI-TPA) film at 725 nm, respectively. (b) and (d) One cycle current change of the p(DPyNDI-TPA) film at 715 nm and the p(NDI-TPA) film at 725 nm, respectively. The response time was calculated at 90% of the full switch because it is difficult to

perceive any further color change with the naked eye beyond this point. All the films were deposited on FTO substrates and tested in CH_2Cl_2/ACN (4:1) solution containing 0.1 M $LiClO_4$.

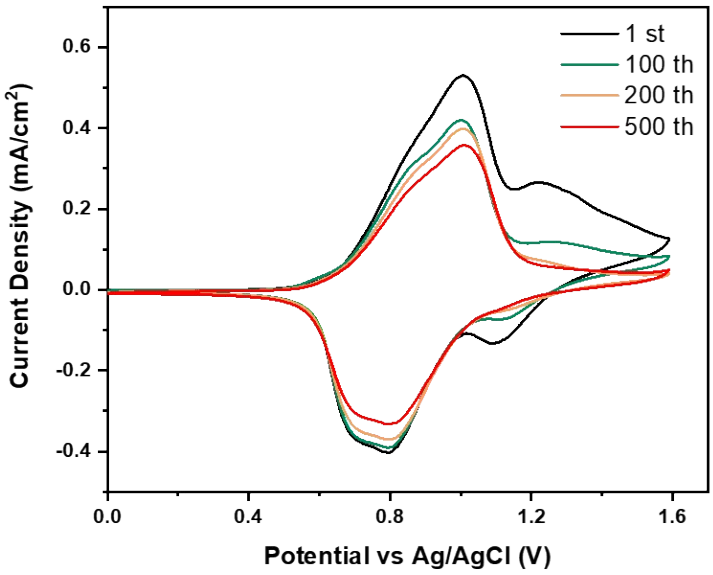

Fig. S9. CV diagrams of p(DPyNDI-TPA) film upon repeated cycling at the rate of 50 mV/s at a potential range from 0.0 V to 1.6 V.

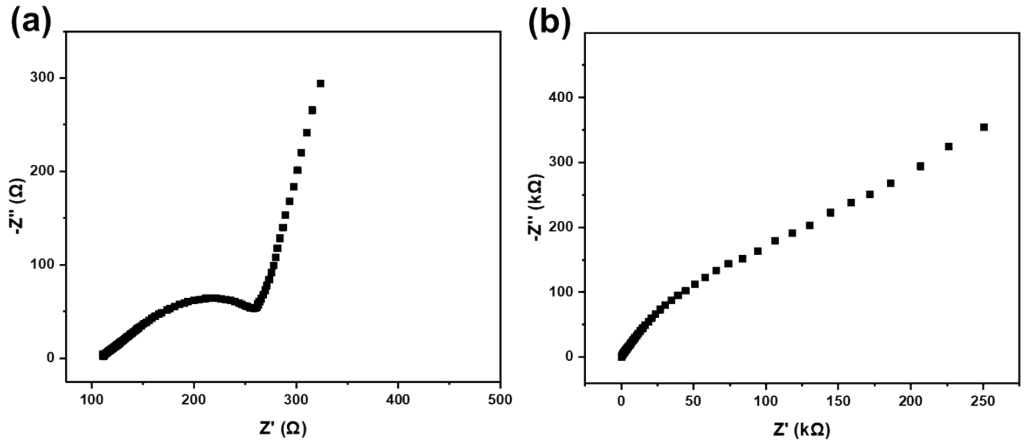

Fig. S10. (a) EIS spectra (Nyquist Plot) of p(DPyNDI-TPA) (a) and p(NDI-TPA) (b) films.

DFT calculation

DFT calculations were performed by the B3LYP/6-311G(d) basis set through Gaussian 09W program.

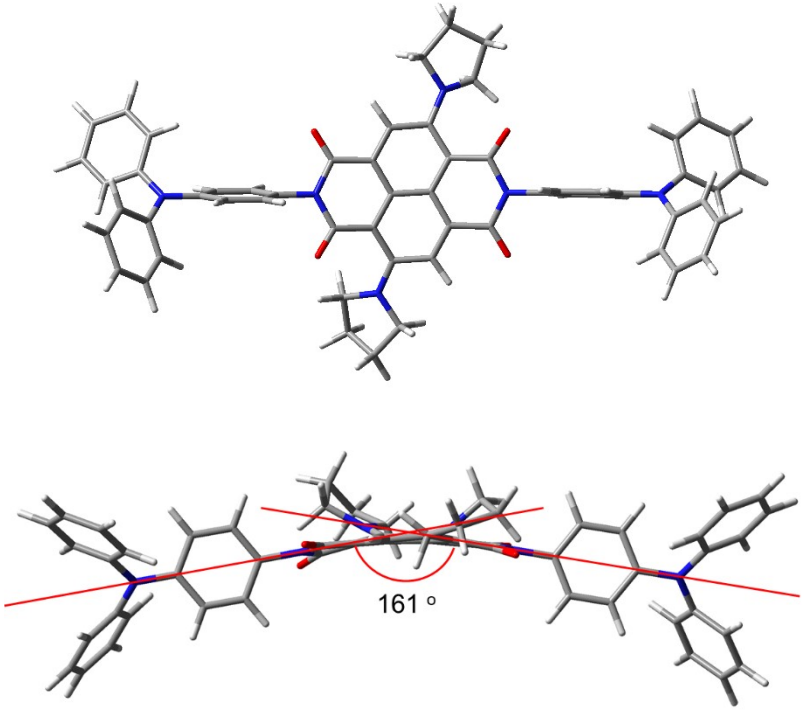

Fig. S11. Optimized structure of DPyNDI-TPA. Top: from the front of view; Bottom: from the side of view.

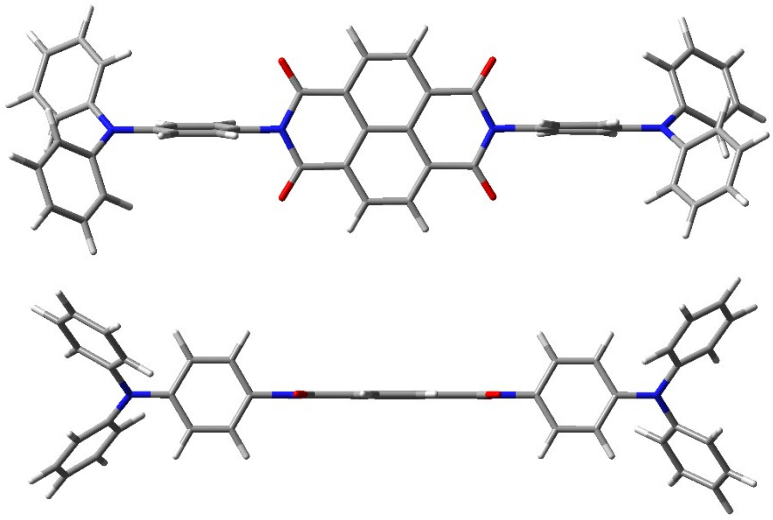

Fig. S12. Optimized structure of NDI-TPA. Top: from the front of view; Bottom: from the side of view.

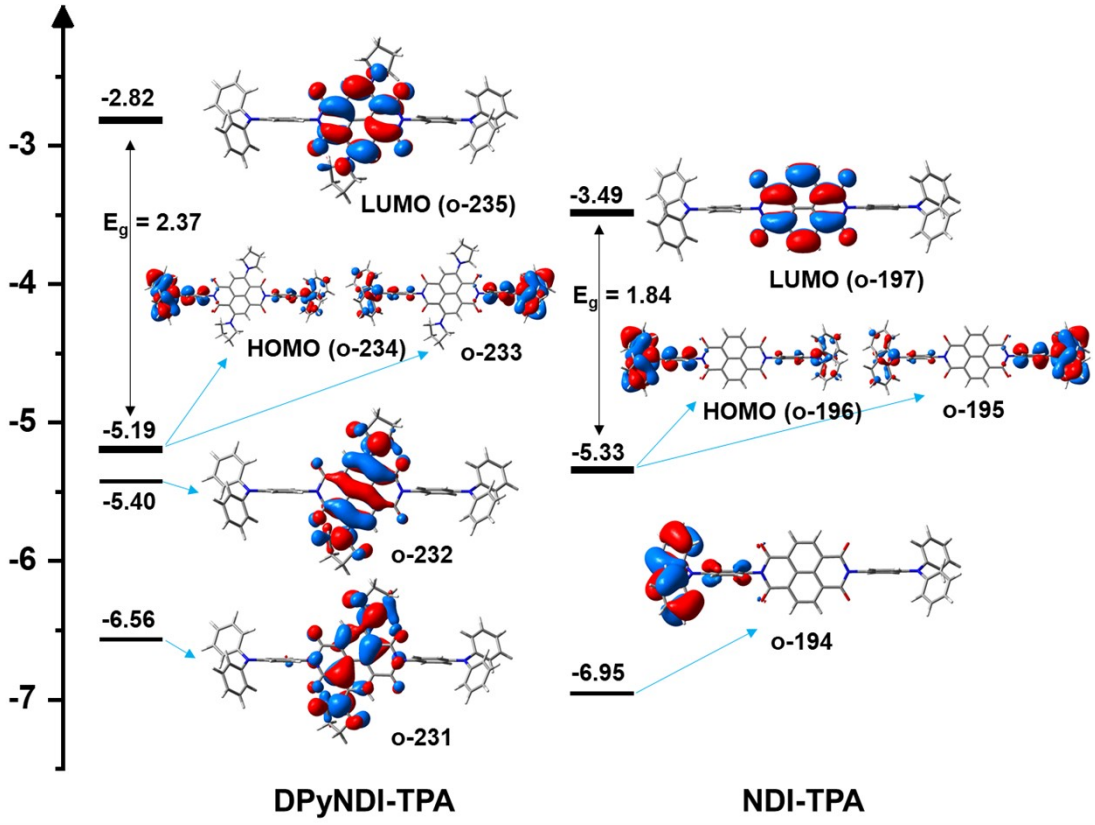

Fig. S13. Frontier molecular orbitals of DPyNDI-TPA and NDI-TPA.

Hirshifeld orbital component analysis

Table S1 The percentage of each atom in defined orbital.

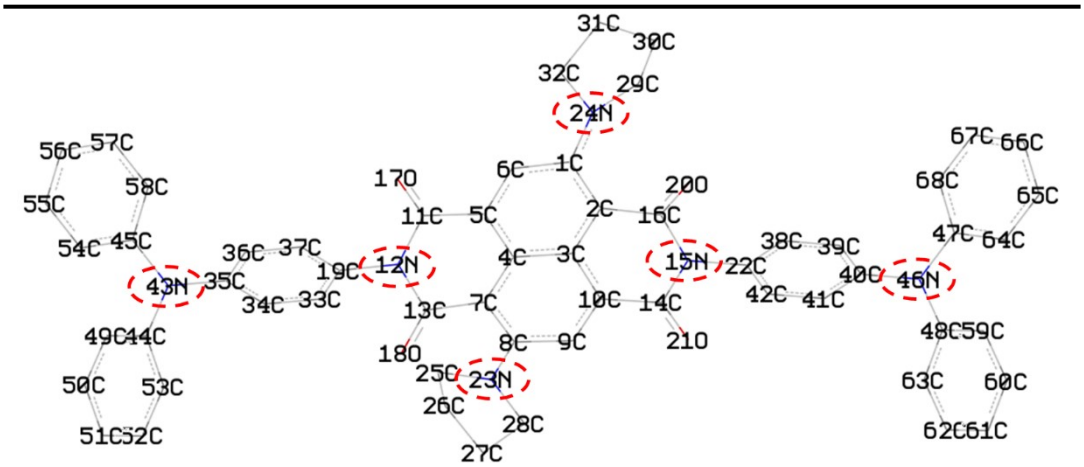

Atom number	Orbit 234	Orbit 233	Orbit 232
1C	0.016%	0.018%	5.602%
2C	0.006%	0.029%	6.998%
3C	0.017%	0.008%	4.720%
4C	0.014%	0.003%	4.802%
5C	0.034%	0.004%	2.416%
6C	0.022%	0.007%	3.791%
7C	0.072%	0.004%	6.778%
8C	0.045%	0.007%	5.208%
9C	0.021%	0.013%	3.546%
10C	0.021%	0.025%	2.340%
11C	0.266%	0.004%	0.491%

12N	0.599%	0.006%	0.175%
13C	0.254%	0.003%	1.475%
14C	0.006%	0.233%	0.475%
15N	0.007%	0.525%	0.184%
16C	0.004%	0.246%	1.498%
17O	0.227%	0.003%	0.739%
18O	0.209%	0.003%	1.963%
19C	5.951%	0.061%	0.033%
20O	0.004%	0.239%	1.889%
21O	0.007%	0.194%	0.733%
22C	0.061%	5.791%	0.024%
23N	0.052%	0.004%	12.772%
24N	0.021%	0.006%	15.608%
25C	0.011%	0.001%	1.530%
26C	0.003%	0.000%	0.345%
27C	0.001%	0.000%	0.184%
28C	0.006%	0.000%	1.419%
29C	0.003%	0.003%	1.868%
30C	0.000%	0.000%	0.354%
31C	0.000%	0.000%	0.225%
32C	0.002%	0.000%	1.734%
33C	1.497%	0.015%	0.011%
34C	4.929%	0.051%	0.008%
35C	4.958%	0.050%	0.010%
36C	5.025%	0.051%	0.027%
37C	1.519%	0.015%	0.011%
38C	0.016%	1.474%	0.008%
39C	0.053%	4.916%	0.011%
40C	0.052%	4.894%	0.002%
41C	0.050%	4.888%	0.005%
42C	0.015%	1.460%	0.011%
43N	22.533%	0.232%	0.069%
44C	4.848%	0.050%	0.015%
45C	4.912%	0.051%	0.018%
46N	0.237%	22.685%	0.005%
47C	0.051%	4.946%	0.002%
48C	0.051%	4.956%	0.001%
49C	4.717%	0.049%	0.015%
50C	1.498%	0.015%	0.004%
51C	5.811%	0.060%	0.018%
52C	1.485%	0.015%	0.005%
53C	4.720%	0.049%	0.013%
54C	4.764%	0.049%	0.016%
55C	1.526%	0.016%	0.006%
56C	5.905%	0.061%	0.020%
57C	1.505%	0.016%	0.005%
58C	4.788%	0.049%	0.016%
59C	0.050%	4.784%	0.001%
60C	0.016%	1.530%	0.000%
61C	0.061%	5.921%	0.001%
62C	0.016%	1.517%	0.001%
63C	0.050%	4.792%	0.001%
64C	0.050%	4.830%	0.001%
65C	0.016%	1.538%	0.001%
66C	0.062%	5.978%	0.002%
67C	0.016%	1.529%	0.000%
68C	0.050%	4.835%	0.002%

Table S2 Electrochromic properties of the compounds in previous literature.

Compounds	λ_{abs} (nm)	Δ%T	t_c[a] (s)	t_b[a] (s)	CE[b] (cm²/C)	Year
P(T-TPA-C)[6]	711	57%	2.5	1.4	196	2015
P(TPA-2Cz)[7]	730	60%	6.1	2.2	59	2015
TPA-PTPI[5]	715	58%	3.3	4.6	371	2017
T-3(CONH-TPA)[8]	715	55%	6.6	5.3	82	2018
TPA-PMDI[9]	740	87%	14.4	6.9	122	2018
p-Benz-3TPA[10]	790	71%	0.8	1.1	294	2018
PTPAFc[11]	800	59%	2.2	2.1	127	2019
COF_{3PA-TT}[12]	1300	41%	18	13	152	2019
CuTCA MOFs[13]	700	65%	4.8	3.3	--	2020
$COF_{TPDA-PDA}$[14]	1050	52%	1.3	0.7	320	2021
p(DPyNDI-TPA)	715	81%	1.45	1.22	306	This work

[a] t_c and t_b refer to the coloring time and bleaching time, respectively. [b] Coloration efficiency (CE) = $\Delta OD/Q_d$.

References

1 S. Ming, S. Zhen, K. Lin, L. Zhao, J. Xu, B. Lu, *ACS Appl. Mater. Interfaces,* 2015, **7**, 11089-11098.
2 Z. Feng, D. Mo, Z. Wang, S. Zhen, J. Xu, B. Lu, S. Ming, K. Lin, J. Xiong, *Electrochim. Acta,* 2015, **160**, 160-168.
3 L. Qian, X. Lv, M. Ouyang, A. Tameev, K. Katin, M. Maslov, Q. Bi, C. Huang, R. Zhu, C. Zhang, *ACS Appl. Mater. Interfaces,* 2018, **10**, 32404-32412.
4 Z. Guo, D. K. Panda, K. Maity, D. Lindsey, T. G. Parker, T. E. Albrecht-Schmitt, J. L. Barreda-Esparza, P. Xiong, W. Zhou, S. Saha, *J. Mater. Chem. C,* 2016, **4**, 894-899.
5 S.-H. Hsiao, Y.-Z. Chen, *Dyes Pigments,* 2017, **144**, 173-183.
6 S.-H. Hsiao, Y.-T. Chiu, *RSC Adv.,* 2015, **5**, 90941-90951.
7 S.-H. Hsiao, J.-C. Hsueh, *J. Electroanal. Chem.,* 2015, **758**, 100-110.
8 S.-H. Hsiao, Y.-Z. Chen, *Eur. Polym. J.,* 2018, **99**, 422-436.
9 S.-H. Hsiao, W.-K. Liao, G.-S. Liou, *Polym. Chem.,* 2018, **9**, 236-248.
10 D. C. Santra, S. Nad, S. Malik, *J. Electroanal. Chem.,* 2018, **823**, 203-212.
11 X. Lv, C. Huang, A. Tameev, L. Qian, R. Zhu, K. Katin, M. Maslov, A. Nekrasov, C. Zhang, *Dyes Pigments,* 2019, **163**, 433-440.
12 Q. Hao, Z. J. Li, C. Lu, B. Sun, Y. W. Zhong, L. J. Wan, D. Wang, *J. Am. Chem. Soc.,* 2019, **141**, 19831-19838.
13 J. Liu, X. Y. Daphne Ma, Z. Wang, L. Xu, T. Xu, C. He, F. Wang, X. Lu, *ACS Appl. Mater. Interfaces,* 2020, **12**, 7442-7450.
14 Q. Hao, Z.-J. Li, B. Bai, X. Zhang, Y.-W. Zhong, L.-J. Wan, D. Wang, *Angew. Chem. Int. Ed.,* 2021, **60**, 12498-12503.